

## Measurement of the Coulomb energy loss by fast protons in a plasma target

G. Belyaev, M. Basko, A. Cherkasov, A. Golubev, A. Fertman, I. Roudskoy,  
S. Savin, B. Sharkov, and V. Turtikov

*Institute for Theoretical and Experimental Physics, B. Cheremushkinskaya 25, 117259 Moscow, Russia*

A. Arzumanov, A. Borisenko, I. Gorlachev, and S. Lysukhin

*Institute for Nuclear Physics, National Nuclear Center of Kazakhstan, 480082 Alma-Ata, Kazakhstan*

D. H. H. Hoffmann and A. Tauschwitz

*Gesellschaft für Schwerionenforschung (GSI), Postfach 110552, D-64220 Darmstadt, Germany*

(Received 6 October 1995)

We report measurements of the energy loss by 1-MeV protons in a plasma target created by electric discharge in the hydrogen gas. Combined with independent measurements of the mean ionization degree and the electron areal density of the plasma column, based on two-wavelength laser interferometry, the energy-loss data let us infer the value of the Coulomb logarithm:  $L_{fe} = 14.9 \pm 2.8$  for the stopping power of the free plasma electrons. This value is  $3.1 \pm 0.6$  times higher than that given by the Bethe formula for the neutral hydrogen and, within the experimental errors, agrees with the theoretical predictions.

PACS number(s): 52.40.Mj, 34.50.Bw

### I. INTRODUCTION

The investigation of the interaction of ionizing radiation with matter has always been a classical topic of atomic and nuclear physics. Due to a wide range of applications, there still is a growing need for a deeper understanding of physical processes that determine the stopping of fast ions in matter.

A large amount of experimental data have been accumulated concerning the stopping of fast ions in cold matter under normal conditions, when the energy loss is dominated by inelastic collisions with bound electrons [1]. At the same time, very few data have been obtained on stopping of ions in plasmas, where the theory predicts a considerable enhancement of the Coulomb energy losses in collisions with free plasma electrons. This provides the principal motivation for the present work.

Assuming that the beam of fast ions is sufficiently dilute and no collective processes such as the beam-plasma instability contribute to the stopping, the beam energy losses can be evaluated in the single-particle approximation.

In general, the Coulomb stopping power of partially ionized matter for a pointlike ion can be represented as the sum of contributions due to bound electrons (be), free plasma electrons (fe), and free plasma ions (fi):

$$\frac{dE}{dx} = \left[ \frac{dE}{dx} \right]_{be} + \left[ \frac{dE}{dx} \right]_{fe} + \left[ \frac{dE}{dx} \right]_{fi}. \quad (1)$$

In the nonrelativistic limit, ignoring the usually small contribution due to the plasma ions, the stopping power for our purposes can be written as

$$-\frac{dE}{dx} = \frac{4\pi e^4 \rho N_0}{m_e v^2 A_t} Z_{\text{eff}}^2 \left[ (Z_t - z^*) L_{be} + z^* G \left( \frac{v}{v_e} \right) L_{fe} \right], \quad (2)$$

where  $N_0$  is the Avogadro number,  $Z_t$  and  $A_t$  are, respectively, the atomic number and mass of target atoms,  $\rho$  is the target density,  $z^*$  is the mean ionization degree of the target material,  $v_e$  is the thermal velocity of free target electrons,  $v$  and  $Z_{\text{eff}}$  are, respectively, the velocity and the effective charge of the fast ion.

The Chandrasekhar function  $G(v/v_e)$  originates from averaging the relative velocity of the fast ion with respect to the target electrons over the Maxwellian distribution. The value of  $G$  approaches unity for  $v \gg v_e$ —which is always the case for situations considered below—and goes to zero as  $(v/v_e)^3$  at  $v \ll v_e$ .

The Coulomb logarithms  $L_{be}$  and  $L_{fe}$  for the bound and free electrons, respectively, appear as a result of integration of the Rutherford cross section over the relevant range of impact parameters or, equivalently, over the relevant range of transferred momenta. In general, when  $L \gg 1$ , the Coulomb logarithm can be expressed as  $L = \ln(p_{\text{max}}/p_{\text{min}})$ , where  $p_{\text{max}} = 2m_e v$  is the maximum transferred momentum, and  $p_{\text{min}}$  is the minimum transferred momentum below which the Rutherford formula becomes inapplicable due to either atomic binding or plasma screening.

In contrast to  $p_{\text{max}}$ , calculation of  $p_{\text{min}}$  is not trivial, and the answer depends on whether the classical or quantum limit applies to the Coulomb scattering of target electrons by the fast ion. The division line between the

classical and quantum domains, controlled by the value of the dimensionless parameter

$$\frac{p_{\min,q}}{p_{\min,cl}} = \frac{\hbar v}{\gamma e^2 Z_{\text{eff}}} = 0.561 \frac{\hbar v}{e^2 Z_{\text{eff}}},$$

is illustrated in Fig. 1 (note that  $Z_{\text{eff}}$  is also a function of  $v$ ); here  $\ln \gamma = 0.577, \dots$  is the Euler constant. Our case, corresponding to protons with the energy  $E \simeq 1$  MeV, falls well into the quantum domain. Hence, we should use the Bethe [2] formula

$$L_{\text{be}} = \ln \frac{2m_e v^2}{\hbar \bar{\omega}} \quad (3)$$

for the Coulomb logarithm of the bound electrons. Here  $\hbar \bar{\omega}$  is the mean excitation energy; for the atomic hydrogen Bethe calculated  $\hbar \bar{\omega} = 1.105$  Ry.

As was shown explicitly by Larkin [3], the Coulomb logarithm  $l_{\text{fe}}$  corresponding to the stopping on free plasma electrons is given by the same Bethe formula (3), but with the mean atomic frequency  $\bar{\omega}$  replaced by the plasma frequency  $\omega_p = (4\pi n_e e^2 / m_e)^{1/2}$ :

$$L_{\text{fe}} = \ln \frac{2m_e v^2}{\hbar \omega_p} \quad (4)$$

A more thorough analysis of the stopping power for the extreme cases of a fully neutral ( $z^* = 0$ ) gas and a fully ionized ( $z^* = Z_i$ ) plasma reveals two main effects.

(1) In low-density plasmas, typical for gas discharges, the values of the plasma frequency  $\omega_p$  are much lower than the atomic frequency  $\bar{\omega}$ , i.e., free electrons "feel" a passing projectile at much larger impact parameters (or, equivalently, at much lower transferred momenta). As a result, as can be seen from Eqs. (2)–(4), the ionization of gases leads to the increase of their stopping powers merely because  $L_{\text{fe}} > L_{\text{be}}$ .

(2) The second effect cannot be seen from Eq. (2). The dynamic equilibrium between the ionization and the electron capture processes for a projective ion is different in

cold and ionized matter because the cross section to capture a free electron is usually much lower than the cross section to capture a bound electron. As a result, the effective charge  $Z_{\text{eff}}$  of a projectile passing through a fully ionized gas is shifted to higher values, causing a further enhancement of the energy loss rate [5].

Following the theoretical studies of the energy-loss mechanisms of fast ions in ionized matter at high temperatures [4–6], an active experimental work was initiated in this field. The first experimental evidence for the enhancement of the stopping power in a plasma was obtained for deuterons and protons [7,8]. Later, systematic measurements of the energy loss by heavy ions in a hydrogen plasma confirmed at a much higher confidence level the enhanced stopping in plasma targets [9–13]. The experiments have been performed at energies between 1 and 6 MeV/u, i.e., in the limit  $v \gg v_e$ , for a large variety of ion species from carbon to uranium. In all cases, however, the measurements yielded the combined effect of the two principal mechanisms of the stopping enhancement [see Eq. (2)], with no quantitative distinction between the individual contributions of each of them.

At low kinetic energies, where the projectile velocity  $v$  becomes comparable to the thermal velocity of the plasma electrons  $v_e$ , the increase in the energy loss rate is expected to be even more dramatic [14,15]. In this case, the main contribution to the enhanced stopping power for heavy ions in a plasma is believed to be caused by significantly higher values of the effective charge  $Z_{\text{eff}}$ , owing to the reduced recombination rate in ionized gases [5,16].

The main goal of the present experiment was to measure separately the enhancement in the Coulomb stopping of fast ions in a plasma due only to the increase of the Coulomb logarithm, i.e., to measure directly the value of the Coulomb logarithm of free electrons  $L_{\text{fe}}$  in a hydrogen plasma. To this end, 1-MeV protons have been chosen as projectile ions because their effective charge  $Z_{\text{eff}} = 1$  remains essentially the same in cold and ionized gases.

## II. DESCRIPTION OF THE EXPERIMENT

Consider two different states of a gaseous hydrogen target: a cold neutral state and a hot partially ionized one. One readily estimates that for 1-MeV protons propagating in a gas with temperature below 500 eV the effective charge  $Z_{\text{eff}} = 1$  and  $G(v/v_e) = 1$ . Then, as can be seen from Eq. (2), the energy loss  $dE$  in the cold hydrogen is directly proportional to the product of the Coulomb logarithm by the areal density of the gas column,

$$-dE_c = \text{const} \times L_{\text{bec}} n_{\text{bec}} dx, \quad (5)$$

whereas the loss in the partially ionized case is

$$-dE_p = \text{const} \times (L_{\text{bep}} n_{\text{bep}} dx + L_{\text{fe}} n_{\text{fe}} dx); \quad (6)$$

here  $n_{\text{bec}}$ ,  $n_{\text{bep}}$ , and  $n_{\text{fe}}$  are, respectively, the number densities of the bound electrons in the cold case, and of the

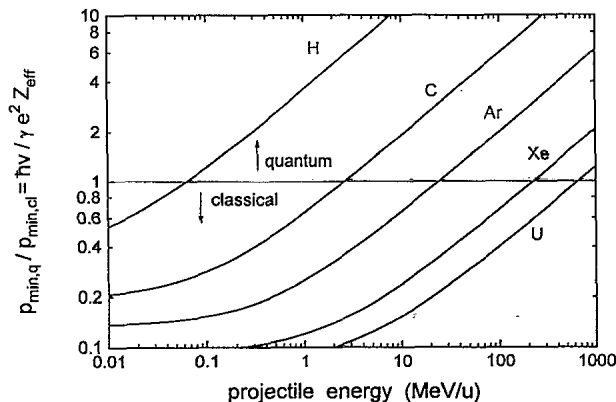


FIG. 1. Classical and quantum limits for the Coulomb scattering of free electrons by different fast ion species moving with different kinetic energies. It is assumed that each ion has the equilibrium effective charge value  $+eZ_{\text{eff}}$ , which is a function of its velocity.

bound and free electrons in the partially ionized target. To be rigorous, we distinguish between the Coulomb logarithm for the cold molecular hydrogen,  $L_{\text{bec}}$  ( $\hbar\bar{\omega} = 18.5$  eV [1]), and that for the atomic hydrogen,  $L_{\text{bep}}$  ( $\hbar\bar{\omega} = 15.0$  eV), in the partially ionized plasma.

Since the plasma areal density  $n_e dx = (n_{\text{fe}} + n_{\text{bep}}) dx$  and its degree of ionization both change in time during the electron discharge, an important issue for the experiment is the time control of (1) the plasma areal density  $n_e dx$ , (2) the plasma ionization degree  $z^*$ , and (3) the contamination of the plasma volume by heavy impurities due to the evaporation of electrode material in the electrical discharge.

To ensure correct experimental measurements of the Coulomb logarithm within a  $\lesssim 10\%$  error bar, the following important requirements regarding the plasma target, the diagnostics, and the beam stability are to be fulfilled.

(1) The energy loss  $dE$  in the target has to be less than the initial projectile energy  $E$  and, at the same time, to exceed by at least a factor of 10 the stability limit  $\delta E$  for the beam energy provided by the accelerator. Also, the energy loss should significantly exceed the resolution threshold of the energy analyzing apparatus. For 1-MeV protons, a hydrogen gas target with an areal density of  $n_H dx \approx n_e dx \sim 10^{18} \text{ cm}^{-2}$  is a suitable choice.

(2) Since 1-MeV protons, passing through a hydrogen target with the areal density of  $\sim 10^{18} \text{ cm}^{-2}$ , would lose some 3 keV of their energy, the energy stability of the beam has to be about  $\delta E/E \approx \pm 100 \text{ eV}/(1 \text{ MeV}) \approx \pm 1 \times 10^{-4}$ .

(3) The energy resolution of the beam energy diagnostics in reality should be not worse than 10% of the energy loss; in reality, the resolution of about 200 eV has been provided.

#### A. Accelerator

The requirements for the ion beam have been fulfilled by using the UKP-2 tandem accelerator at the Kazakh Institute for Nuclear Physics in Alma-Ata [17]. During the experiments, the stability of the accelerating voltage was maintained at the level of  $\pm 100$  V.

The plasma target was integrated into the high vacuum system of the beam line. Differential pumping at a rate of 300 l/s proved to be sufficient in insulating the vacuum beam line from the pressurized target during its operating cycle.

#### B. Plasma target

The plasma was generated by igniting an electric discharge in two collinear quartz tubes, each of 6 mm in diameter and 78 mm long (see Fig. 2).

The capacitor bank of  $3 \mu\text{F}$ , discharged at voltages 2–4 kV, produces the electric current of 3 kA flowing in two opposite directions in either of the two quartz tubes. Such a design for the plasma target enables us to suppress the well-known effect of the plasma lens [18] caused by the magnetic field of the current: the focusing effect of the first discharge tube is compensated for by the de-

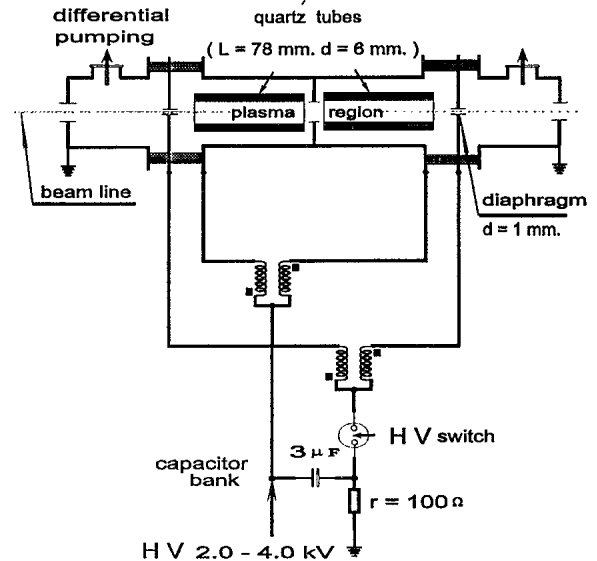


FIG. 2. Principal scheme of the plasma target used in the experiment.

focusing effect of the second one. Symmetry of the discharge is ensured by special inductivity coils, included into the discharge circuit, with two wires for the two current branches wound in the opposite directions. For the initial pressure of the hydrogen gas ranging from 200 to 900 Pa (2–9 mbar), the plasma electron density of up to  $10^{17} \text{ cm}^{-3}$  can be created in such a discharge.

The discharge current oscillates with a half period of  $\sim 5 \mu\text{s}$ , which agrees fairly well with the calculated lifetime of the hydrogen plasma, spilling out of the tube ends in the course of the hydrodynamic expansion.

#### C. Plasma diagnostics

According to Eqs. (5) and (6), the essential parameters to be measured in the experiment are the areal density of the free electrons and the degree of ionization. The measurements have been performed by using the method of time-resolved two-wavelength Mach-Zehnder interferometry in axial direction. Only the plasma region where the proton beam passes—i.e., the region of 1 mm in diameter and 150 mm long—has been probed. The electron areal density in this region is assumed to be independent of radius, as is confirmed by the parallel lines of the interferometric pattern in the streak images. The optical setup for the Mach-Zehnder interferometer with two lasers (He-Ne with  $\lambda_1 = 0.63 \mu\text{m}$  and He-Cd with  $\lambda_2 = 0.44 \mu\text{m}$ ) is displayed in Fig. 3. Streak images of the interferometric fringes have been recorded with the streak-camera FER-7. The dimensionless shifts of fringes  $k_1$  and  $k_2$  with respect to the neutral-gas target state, determined by the refraction index of matter along the target axis, can be expressed as linear combinations of the areal densities of the bound and free electrons along the line of sight,

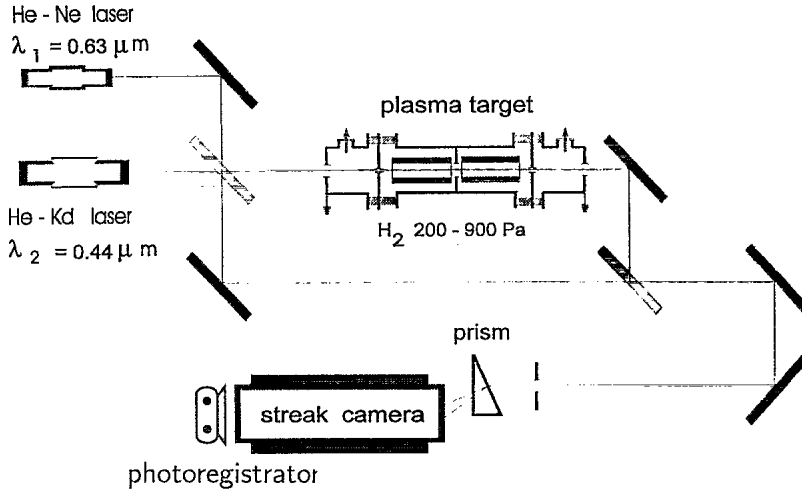


FIG. 3. Optical scheme of the two-wavelength Mach-Zehnder interferometry plasma diagnostics.

$$k_1 = \frac{1}{\lambda_1} C_H (n_{\text{bep}} dx - n_{\text{bec}} dx) - \lambda_1 C_e n_{\text{fe}} dx, \quad (7)$$

$$k_2 = \frac{1}{\lambda_2} C_H (n_{\text{bep}} dx - n_{\text{bec}} dx) - \lambda_2 C_e n_{\text{fe}} dx, \quad (8)$$

where

$$C_H = 0.51 \times 10^{-23} \text{ cm}^3, \quad C_e = 4.48 \times 10^{-14} \text{ cm}.$$

Having measured the values of  $k_1$  and  $k_2$ , we can calculate the quantities

$$n_{\text{fe}} dx = \frac{1}{C_e} \frac{k_2 \lambda_2 - k_1 \lambda_1}{\lambda_2^2 - \lambda_1^2} \quad (9)$$

and

$$\frac{k_2^0}{k_1^0} = \frac{C_H(1-\alpha) - \lambda_2^2 C_e \alpha}{C_H(1-\alpha) - \lambda_1^2 C_e \alpha} \frac{\lambda_1}{\lambda_2}, \quad (10)$$

where

$$\alpha = \frac{n_{\text{fe}} dx}{n_{\text{fe}} dx + n_{\text{bep}} dx} \quad (11)$$

is the mean degree of ionization, and

$$k_1^0 = k_1 + \frac{1}{\lambda_1} C_H n_{\text{bec}} dx, \quad k_2^0 = k_2 + \frac{1}{\lambda_2} C_H n_{\text{bec}} dx. \quad (12)$$

The values of  $n_{\text{bec}} dx$  were determined experimentally by measuring the proton energy losses in the cold target state. As a result, the two-wavelength method gives us the possibility to monitor the temporal evolution of the plasma areal electron density and the mean degree of ionization.

#### D. Energy-loss diagnostic line

To carry out measurements of the proton energy losses, the following diagnostic system has been developed. The diagnostic line, shown in Fig. 4, consists of the following sequence of the beam-optics elements positioned along the proton beam path behind the plasma target: the entrance slit S1, the bending magnet with a deflection of  $45^\circ$  over the radius of 1.5 m, the electrostatic deflector, which deflects the beam in the horizontal plane, and the quadrupole electrostatic lens. Behind the 0.1-mm slit S2 that can be shifted perpendicular to the incoming beam a 1-mm-thick plastic scintillator is placed. The scintillator is

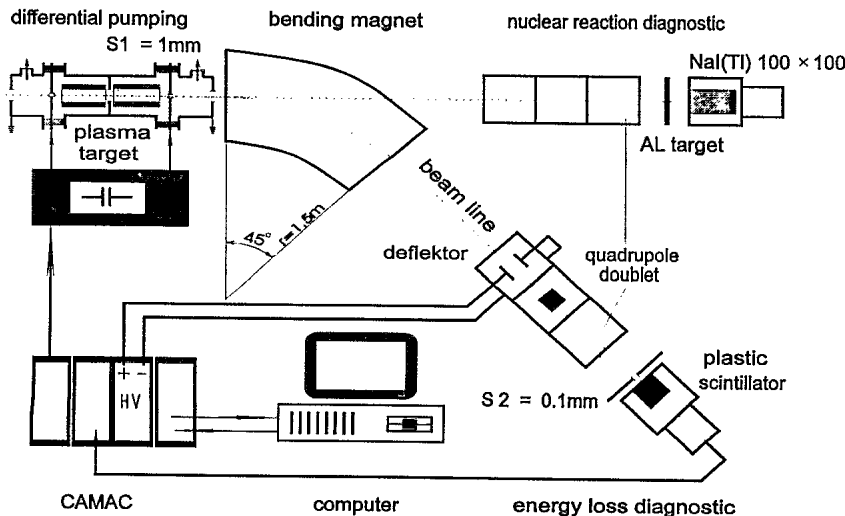


FIG. 4. Scheme of the diagnostic line for measuring the proton energy losses.

connected to a photomultiplier by the fiber optics. The signals are digitized with the 10-MHz analog-to-digital converter and stored in the computer.

In the present experiment the diagnostic line with the  $L = 450$  cm separation between the slits S1 and S2 was used, which let us achieve a high-energy resolution of  $\delta E/E \approx 0.02\%$  at  $E = 1$  MeV.

The beam deflection in the bending magnet depends on the value of the proton energy coming out of the target. If the protons lose a certain energy  $dE$  in the target, the beam is displaced by a certain distance  $dx$  against the diagnostic slit S2, with  $dx$  being directly proportional to  $dE$ . At the same time, this displacement can be reverted by applying an appropriate voltage  $U$  to the electrostatic deflector. Apparently, the applied voltage  $U$  is also directly proportional to the proton energy loss  $dE$ .

To determine experimentally the relationship between the deflection potential  $U$  and the energy loss  $dE$ , we made use of the standard technique based on the resonant reaction  $^{27}\text{Al}(p, \gamma) \rightarrow ^{28}\text{Si}$  ( $E_r = 991.9 \pm 0.05$  keV) that is regularly available at the UKP-2 accelerator. The  $\gamma$  photons were detected with the NaI (TI) scintillator. Proton energy variations caused by the variations of the hydrogen gas pressure have been compensated for by an appropriate voltage applied to the casing of the  $^{27}\text{Al}$  target; this voltage served as the measure of the proton energy loss  $dE$ . The calibration curve obtained in this manner is shown in Fig. 5. The same measurements were used to determine the areal density of the bound electrons  $n_{\text{bec}} dx$ .

Each measurement of the proton energy loss  $dE$  in the plasma was based on measuring the intensity of the proton beam during the discharge at a fixed value of the deflector potential  $U$ . The beam current fluctuations due to the instability of the proton source were suppressed by averaging over a series of 50 shots. Then, the measurement was repeated for the next value of the deflector potential  $U$ , with an increment corresponding to a  $dE \approx 560$  eV change in the proton energy. In this way, the entire

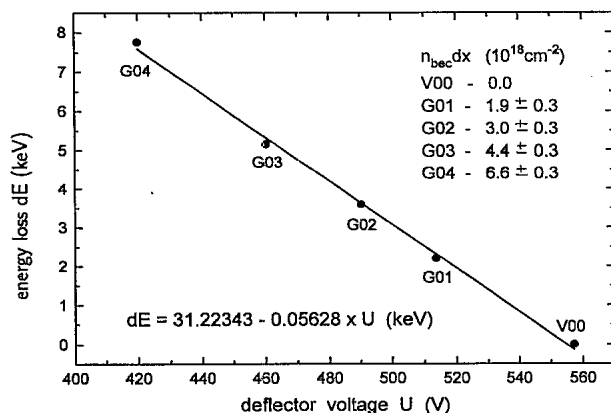


FIG. 5. Calibration curve for the relationship between the proton energy loss  $dE$  and the deflector voltage  $U$ . This same plot gives  $dE$  as a function of the electron areal density  $n_{\text{bec}} dx$  in the cold state of the target.

relevant range of the proton energies was scanned for fixed values of the initial hydrogen pressure and the capacitor bank voltage.

### III. RESULTS OF MEASUREMENTS

Figure 6 shows the processed experimental data for the proton energy losses obtained for a single pair of the values of the initial areal density  $n_{\text{bec}} dx = 3.0 \times 10^{18} \text{cm}^{-2}$  and the capacitor bank voltage 3 keV. The experimental error is determined by the accuracy of measurement of the beam intensity distribution in the plane of the slit S2. The main contribution to the beam spread originates from the finite beam emittance value. Also shown in this figure is the oscillogram of the absolute value of the discharge current flowing through the target. The half period of the current oscillation, equal to  $5 \mu\text{s}$ , delimits the lifetime of the plasma state.

Results of the two-wavelength interferometry, as obtained for the same values of the initial hydrogen pressure and the capacitor voltage, are displayed versus time in Figs. 7 and 8. It is seen that both the areal density of the free electrons  $n_{\text{fe}} dx$  and the mean ionization degree  $\alpha$  achieve maxima at about  $1 \mu\text{s}$  after the ignition of the discharge. We use these maximum values to infer the plasma Coulomb logarithm  $L_{\text{fe}}$ .

By virtue of Eqs. (5), (6), and (11) we can express the ratio between the Coulomb logarithms for the free and bound electrons as

$$\frac{L_{\text{fe}}}{L_{\text{bec}}} = \frac{dE_p}{dE_c^*} - \frac{1-\alpha}{\alpha} \frac{L_{\text{bep}}}{L_{\text{bec}}}, \quad (13)$$

where  $dE_p = 3.8 \pm 0.4$  keV is the proton energy loss in the plasma target at  $1.2 \mu\text{s}$  after the ignition, when the ionization degree  $\alpha = 0.44 \pm 0.1$  is maximum. Here  $dE_c^* = dE_c(n_{\text{fe}} dx)/(n_{\text{bec}} dx)$  is the energy loss in the cold hydrogen with the areal density  $n_{\text{bec}} dx$  numerically equal to the measured areal density  $n_{\text{fe}} dx = (7.2 \pm 0.2) \times 10^{17} \text{cm}^{-2}$  of the free electrons in the plasma state of the tar-

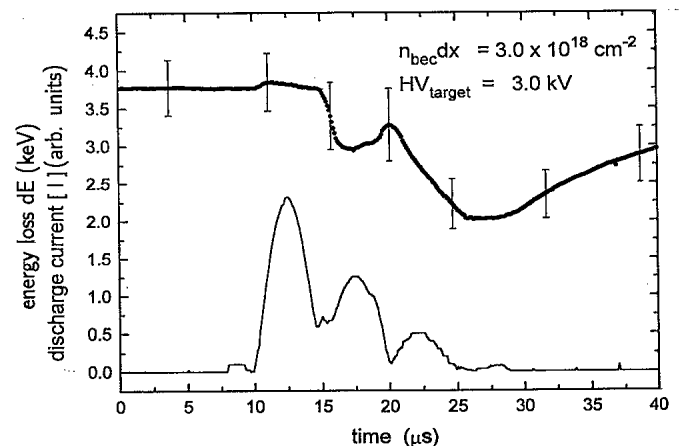


FIG. 6. Plotted as a thick black curve is the temporal behavior of the proton energy loss  $dE_p$  in the plasma target. Shown also is the absolute value (in arbitrary units) of the electric discharge current.

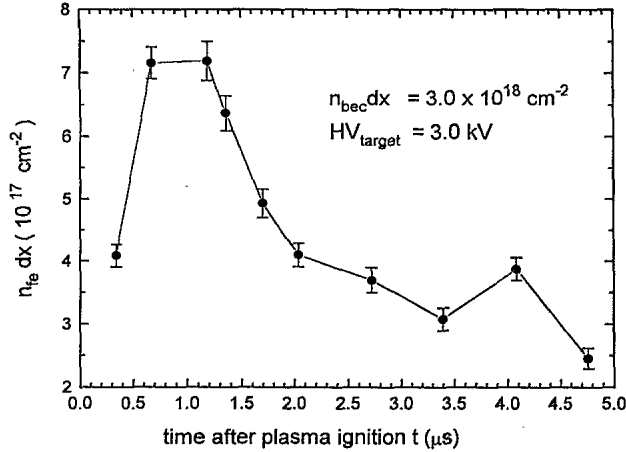


FIG. 7. Areal density of the free plasma electrons along the beam path as a function of time during the first half-period of the discharge current oscillation.

get; it can be easily inferred from the calibration curve in Fig. 5. Finally, evaluating  $L_{\text{bep}}$  and  $L_{\text{bec}}$  from Eq. (3) by substituting  $\hbar\bar{\omega} = 15.0$  eV and  $\hbar\bar{\omega} = 18.5$  eV, respectively, we arrive at

$$\frac{L_{\text{fe}}}{L_{\text{bec}}} = 3.1 \pm 0.6, \quad L_{\text{fe}} = 14.9 \pm 2.8.$$

#### IV. CONCLUSION

We have measured the energy losses by 1-MeV protons in a gaseous hydrogen target in two different states: in the cold state of neutral gas and in the partially ionized plasma state. The parameters of the plasma and beam diagnostics have been aimed at achieving a  $\approx 10\%$  accuracy in measuring such key quantities as the areal densities of the free and bound electrons along the beam path and

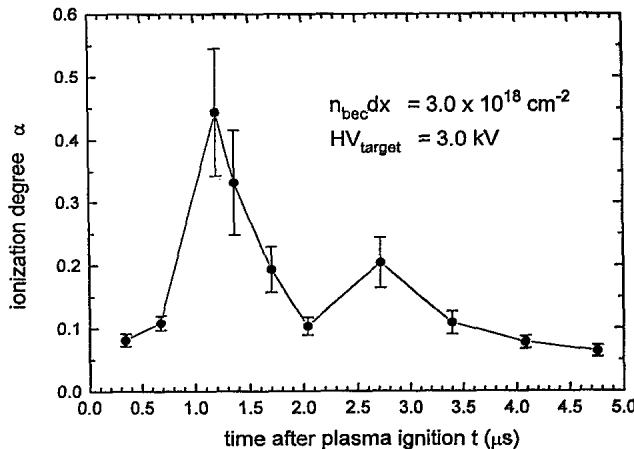


FIG. 8. Mean ionization degree as a function of time during the first half period of discharge current oscillation.

the proton energy loss. The overall target areal density was sufficiently small, so that 1-MeV protons lost no more than 4% of their initial energy and the beam-target interaction could be treated in the monochromatic approximation.

By comparing the energy losses in the cold and ionized target states and assuming that the Coulomb logarithm  $L_{\text{be}}$  for the bound electrons is well known (from both the theory and experiment), we have been able to infer the experimental value of the Coulomb logarithm for the free plasma electrons,  $L_{\text{fe}} = 14.9 \pm 2.8$ . An essential point here is that no effects associated with the variation of the projectile effective charge  $Z_{\text{eff}}$  have interfered with the enhancement of the stopping power due to the target ionization: to a high accuracy,  $Z_{\text{eff}}$  for 1-MeV protons remains equal to 1 independent of the target state. The main source of error in the measured value of  $L_{\text{fe}}$  originates from the measurement of the mean ionization degree in the plasma state of the target.

Our experimental result is to be compared with the theoretical prediction by Larkin [3]:

$$\begin{aligned} L_{\text{fe}} &= \ln \frac{2m_e v^2}{\hbar\omega_p} \\ &= 12.13 + \ln \left[ \left( \frac{E}{1 \text{ MeV}} \right) \left( \frac{10^{17} \text{ cm}^{-3}}{n_{\text{fe}}} \right)^{1/2} \right] \\ &= 12.48. \end{aligned}$$

Note that the above theoretical value is known to an accuracy better than 0.5% because a 10% error in the value of  $n_{\text{fe}}$  (typical for our experimental conditions) results in only a 0.4% error for the theoretical value of  $L_{\text{fe}}$ . Thus, within the experimental errors, no discrepancy has been found between the theory and experiment for the stopping of fast pointlike charges in low-density plasmas.

The results of our experiment have direct implications for the inertial confinement fusion targets driven by the beams of light and heavy ions. In both types of thermonuclear targets the beam absorbing layers usually contain low-density layers of low- $Z$  materials [19], which become fully ionized in the course of ion irradiation. Hence, an adequate modeling of the ion stopping in plasmas is a key element for the target design in the inertial confinement fusion. Also, once the Larkin formula for the stopping power of the free plasma electrons is experimentally verified, the energy losses by fast protons could be employed as a powerful tool for the plasma diagnostics in a number of different types of experiments.

#### ACKNOWLEDGMENTS

This work was supported by NATO Research Grant No. 931324 and by NATO Linkage Grant No. 920584. We wish to thank P. Aristov, A. Eliseev, and A. Platonov for efficient help in this work.

- [1] S. P. Ahlen, *Rev. Mod. Phys.* **52**, 121 (1980).
- [2] H. A. Bethe, *Ann. Phys.* **5**, 325 (1930).
- [3] A. I. Larkin, *Zh. Eksp. Teor. Fiz.* **37**, 264 (1959) [*Sov. Phys. JETP* **37**, 186 (1960)].
- [4] T. A. Mehlhorn, *J. Appl. Phys.* **52**, 6522 (1981).
- [5] E. Nardi and Z. Zinamon, *Phys. Rev. Lett.* **49**, 1251 (1982).
- [6] M. M. Basko, *Fiz. Plazmy*, **10**, 1195 (1984) [*Sov. J. Plasma Phys.* **10**, 689 (1984)].
- [7] F. C. Young *et al.*, *Phys. Rev. Lett.* **49**, 549 (1982).
- [8] J. N. Olsen and T. A. Mehlhorn, *J. Appl. Phys.* **58**, 1251 (1985).
- [9] D. H. H. Hoffmann *et al.*, *Z. Phys. A* **330**, 339 (1988).
- [10] C. Deutsch *et al.*, *Nucl. Instrum. Methods Phys. Res. Sect. A* **278**, 38 (1989).
- [11] D. H. H. Hoffmann *et al.*, *Phys. Rev. A* **42**, 2313 (1990).
- [12] K.-G. Dietrich *et al.*, *Laser Part. Beams* **8**, 583 (1990).
- [13] K.-G. Dietrich *et al.*, *Phys. Rev. Lett.* **69**, 3623 (1992).
- [14] Th. Peter and J. Meyer-ter-Vehn, *Phys. Rev. A* **43**, 1998 (1991).
- [15] J. Jacoby *et al.*, *Phys. Rev. Lett.* **74**, 1550 (1995).
- [16] Th. Peter, R. Arnold, and J. Meyer-ter-Vehn, *Phys. Rev. Lett.* **57**, 1859 (1986).
- [17] A. Arzumanov, A. Borisenko, and S. Lysukhin, in *Proceedings of EPAC-92*, Berlin (Institute of Physics, Bristol, 1992), Vol. 1, p. 495.
- [18] E. Boggasch *et al.*, *Appl. Phys. Lett.* **60**, 2475 (1992).
- [19] D. D.-M. Ho, J. D. Lindl, and M. Tabak, *Nucl. Fusion* **34**, 1081 (1994).